Strain accumulation in sand due to cyclic loading: drained cyclic tests with triaxial extension

T. Wichtmann[i)], A. Niemunis, Th. Triantafyllidis

Institute of Soil Mechanics and Foundation Engineering, Ruhr-University Bochum, Universitätsstraße 150, 44801 Bochum, Germany

Abstract

This paper presents results of numerous drained cyclic tests with triaxial extension. The influence of the strain amplitude, the average stress and the number of load cycles on the accumulation rate was studied. A simple cyclic flow rule was observed. Most findings confirm a previous study with cyclic triaxial compression tests. The test results serve as the basis of an explicit accumulation model.

Key words: Cyclic triaxial tests; triaxial extension; strain accumulation; residual strains; sand

1   Introduction

In order to predict the residual settlements in non-cohesive soils under high-cyclic loading (= number of cycles $N > 10^3$) an explicit accumulation model was developed [1]. The model is based on numerous cyclic triaxial tests [2] and multiaxial Direct Simple Shear (DSS) tests [3]. The cyclic triaxial tests presented in [2] covered uniaxial "in-phase" [1] stress cycles that superposed triaxial compression. At a constant lateral stress σ_3 the axial stress σ_1 was oscillating with an amplitude $\sigma_1^{\mathrm{ampl}} = q^{\mathrm{ampl}}$ about the average value σ_1^{av}. The average deviatoric stress was $q^{\mathrm{av}} = \sigma_1^{\mathrm{av}} - \sigma_3 \geq 0$. The experiments were performed with a uniform medium coarse quartz sand. Tests with a simultaneous oscillation of σ_1 and σ_3 ("off-phase" cycles) were published in [3].

As already shown in [2] for $q^{\mathrm{av}} \geq 0$ the "cyclic flow rule", i.e. the ratio of the accumulated volumetric ($\varepsilon_v^{\mathrm{acc}} = \varepsilon_1^{\mathrm{acc}} + 2\varepsilon_3^{\mathrm{acc}}$) and the accumulated deviatoric ($\varepsilon_q^{\mathrm{acc}} = 2/3(\varepsilon_1^{\mathrm{acc}} - \varepsilon_3^{\mathrm{acc}})$) strain is a simple function of the average stress ratio $\eta^{\mathrm{av}} = q^{\mathrm{av}}/p^{\mathrm{av}}$ only with $p^{\mathrm{av}} = (\sigma_1^{\mathrm{av}} + 2\sigma_3)/3$ being the average mean pressure. The strain amplitude, the average stress and the void ratio do not influence the *direction* of the strain accumulation rate, while some slight changes with the number of cycles occur. In [2] it is demonstrated that the

direction of the strain accumulation rate can be well approximated by the flow rules of constitutive models for monotonous loading (e.g. modified Cam clay model).

The *intensity* of the strain accumulation rate $\dot{\varepsilon}^{\mathrm{acc}} = \partial \varepsilon^{\mathrm{acc}}/\partial N$ with $\varepsilon = \|\boldsymbol{\varepsilon}\| = \sqrt{(\varepsilon_1)^2 + 2(\varepsilon_3)^2}$ was found proportional to the square of the strain amplitude, i.e. $\dot{\varepsilon}^{\mathrm{acc}} \sim (\varepsilon^{\mathrm{ampl}})^2$. The accumulation rate decreases exponentially with the average mean pressure p^{av} and increases exponentially with the average stress ratio $\eta^{\mathrm{av}} = q^{\mathrm{av}}/p^{\mathrm{av}}$. Under cyclic loading a loose soil is compacted faster than a dense one. The relationship $\varepsilon^{\mathrm{acc}} \sim \ln(N)$ holds for $N < 10^4$ while the increase of the accumulated (residual) strain with N is faster than logarithmic for higher numbers of cycles. The loading frequency does not influence the accumulation. Tests on four different grain size distributions demonstrated an increase of $\dot{\varepsilon}^{\mathrm{acc}}$ with an increasing uniformity index $U = d_{60}/d_{10}$ and a decreasing mean grain diameter d_{50} [2].

To the authors' best knowledge drained cyclic *triaxial extension* tests, i.e. tests with an average stress q^{av} lying below the *p*-axis in the *p*-*q*-plane (Fig. 1), have not been presented yet in the literature. This paper presents such tests. Different stress amplitudes q^{ampl} (Section 2.2), average mean pressures p^{av} (Section 2.3) and average stress ratios $\eta^{\mathrm{av}} = q^{\mathrm{av}}/p^{\mathrm{av}}$ (Section 2.4) were tested. The influence of the number of cycles is discussed in Section 2.5. The test results are compared to the triaxial compression tests presented in [2].

[i)]Corresponding author. Tel.: + 49-234-3226080; fax: +49-234-3214150; *e-mail address:* torsten.wichtmann@rub.de
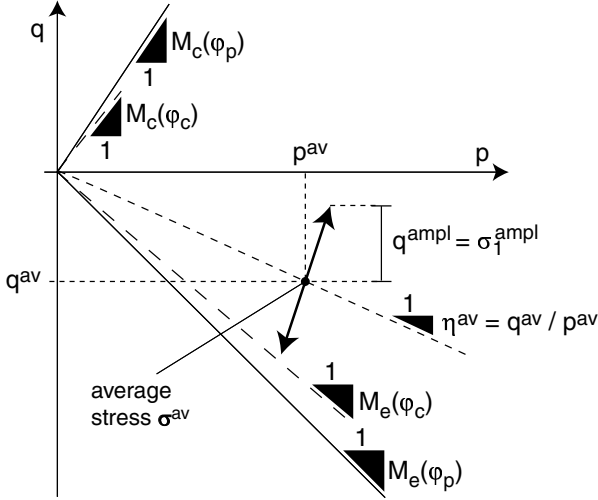
Fig. 1: State of stress in a test with triaxial extension ($M_e(\varphi_c)$, $M_c(\varphi_c)$: inclinations of critical state line, $M_e(\varphi_p)$, $M_c(\varphi_p)$: inclinations of failure line from monotonous tests)

2   Test procedures and results

2.1   Test procedure

In all tests the lateral stress σ_3 was kept constant and the axial component σ_1 was cyclically varied, i.e. only uniaxial "in-phase" stress cycles were tested. The same medium coarse uniform sand ($d_{50} = 0.55$ mm, $U = d_{60}/d_{10} = 1.8$, maximum and minimum void ratios $e_{\max} = 0.874$, $e_{\min} = 0.577$) as in the tests with triaxial compression was used. The grain size distribution is given in [2]. The specimens were prepared by pluviating dry sand out of a funnel through air into half-cylinder moulds and after that saturated by de-aired water. The test device and the measurement technique are described in detail in [2]. In all tests 10,000 cycles were applied with a frequency of $f_B = 0.1$ Hz. This lower frequency compared to the tests in [2] ($f_B = 1$ Hz) was chosen due to technical reasons (adapter for tension loading).

2.2   Influence of the stress/strain amplitude

Seven tests with an identical average stress ($p^{\mathrm{av}} = 200$ kPa, $\eta^{\mathrm{av}} = $ -0.5) and a similar initial density index ($0.59 \leq I_{D0} = (e_{\max} - e)/(e_{\max} - e_{\min}) \leq 0.66$) were performed applying different stress amplitudes 20 kPa $\leq q^{\mathrm{ampl}} \leq 50$ kPa. Figure 2 shows, that the strain amplitude $\varepsilon^{\mathrm{ampl}}$ decreased during the first 100 cycles (this so-called conditioning phase was significant especially in the case of the higher stress amplitudes) and after that remained nearly constant (even a slight re-increase of $\varepsilon^{\mathrm{ampl}}$ was measured for $N > 100$). A similar behaviour was observed for cyclic compression [2]. In Fig. 3 it is shown, that the strain amplitudes $\varepsilon_v^{\mathrm{ampl}}$,

$\varepsilon_q^{\mathrm{ampl}}$, $\varepsilon^{\mathrm{ampl}}$ and $\gamma^{\mathrm{ampl}} = (\varepsilon_1 - \varepsilon_3)^{\mathrm{ampl}}$ are linear proportional to the stress amplitude q^{ampl} for $q^{\mathrm{ampl}} \leq 40$ kPa. For higher stress amplitudes the strain amplitudes increase over-linearly with q^{ampl}.
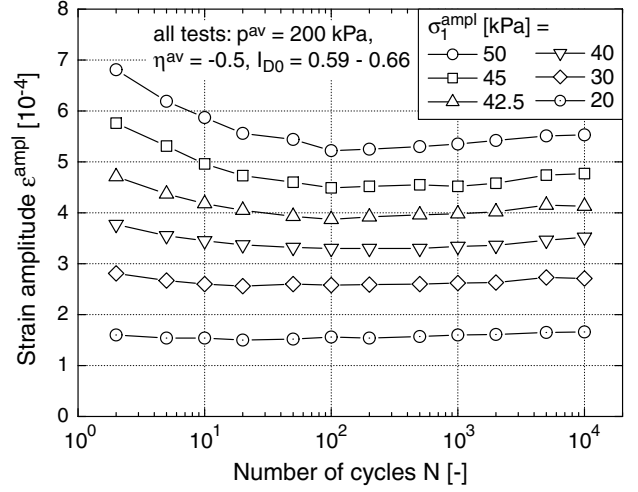
Fig. 2: Strain amplitude $\varepsilon^{\mathrm{ampl}}$ as a function of the number of cycles N for different stress amplitudes q^{ampl}
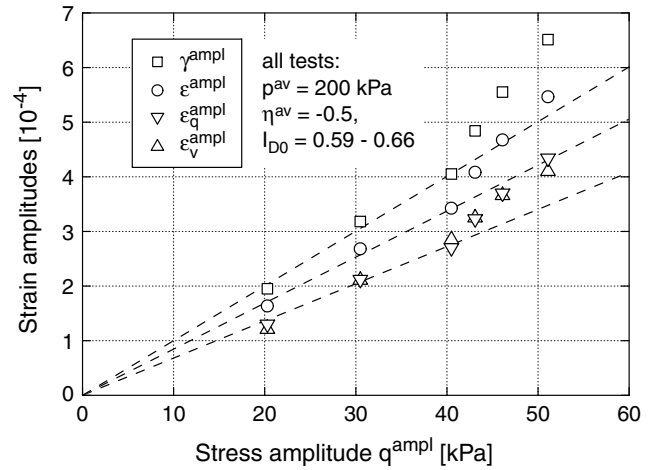
Fig. 3: Strain amplitudes (mean values over 10^4 cycles) in dependence of stress amplitude q^{ampl}

Fig. 4 presents the total accumulation $\varepsilon^{\mathrm{acc}}(N)$. We distinguish between the first, *irregular* cycle and the subsequent *regular* ones since the deformation during the first cycle may significantly differ from that during the following cycles. The *explicit* accumulation model [1] describes the strain due to the regular cycles only. An *implicit* model (a conventional $\boldsymbol{\sigma}$-$\boldsymbol{\varepsilon}$ model) is responsible for the calculation of the irregular cycle. Fig. 4 presents solely the accumulation during the regular cycles. From Fig. 4 it is obvious, that larger stress amplitudes produce higher accumulation rates. The residual strain grows almost proportionally to the logarithm of N, except for the stress amplitudes $q^{\mathrm{ampl}} \geq$

45 kPa, where for $N \geq 2,000$ the accumulation is faster than $\ln(N)$. The function f_N describing the shape of the curves $\varepsilon^{\mathrm{acc}}(N)$ is further discussed in Section 2.5.
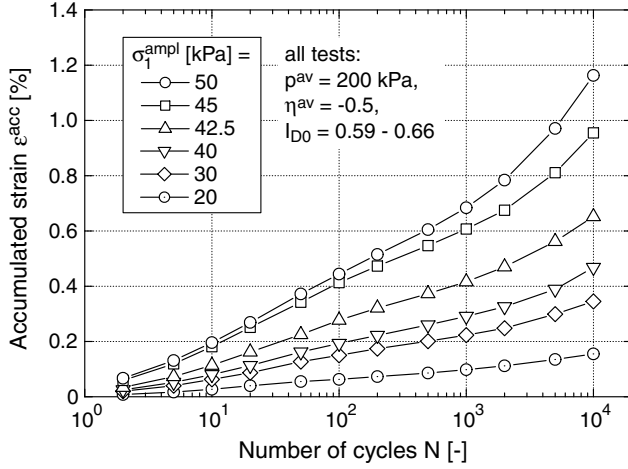
Fig. 4: Accumulation curves $\varepsilon^{\mathrm{acc}}(N)$

In Fig. 5 the residual strain after N cycles is plotted versus the square of the strain amplitude, which was calulated as the mean value $\bar{\varepsilon}^{\mathrm{ampl}} = (\int_1^N \varepsilon^{\mathrm{ampl}}(N) \ \mathrm{d}N)/N$. In order to remove the effect of the slightly varying initial densities and the different compaction rates, $\varepsilon^{\mathrm{acc}}$ has been normalized, separating the influence f_e of the void ratio as proposed in [2]:

$$f_e = \frac{(C_e - e)^2}{1 + e} \frac{1 + e_{\mathrm{ref}}}{(C_e - e_{\mathrm{ref}})^2} \qquad (1)$$

With the material constant $C_e = 0.52$ and the reference void ratio $e_{\mathrm{ref}} = e_{\mathrm{max}} = 0.874$ the function f_e describes the influence of the void ratio e on the intensity of accumulation. In Fig. 5 the bar over f_e indicates that $\bar{f}_e$ has been calculated for a mean value of the evolving void ratio, namely $\bar{e} = (\int_1^N e(N) \ \mathrm{d}N)/N$. Independent of N, the proportionality $\varepsilon^{\mathrm{acc}} \sim (\varepsilon^{\mathrm{ampl}})^2$ turns out to be valid also for triaxial extension. Thus, the function [2]

$$f_{\mathrm{ampl}} = (\varepsilon^{\mathrm{ampl}}/\varepsilon_{\mathrm{ref}}^{\mathrm{ampl}})^2 \qquad (2)$$

with the reference amplitude $\varepsilon_{\mathrm{ref}}^{\mathrm{ampl}} = 10^{-4}$ is assumed valid for all stress states.

Fig. 6 presents the ratio $\omega = \varepsilon_v^{\mathrm{acc}}/\varepsilon_q^{\mathrm{acc}}$ for different numbers of cycles. No significant influence of the strain amplitude $\varepsilon^{\mathrm{ampl}}$ on the direction of strain accumulation was found. This conclusion coincides with [2]. Similarly as in the tests with triaxial compression, a slight increase of the volumetric component of the direction of strain accumulation with N was observed (Fig. 6).
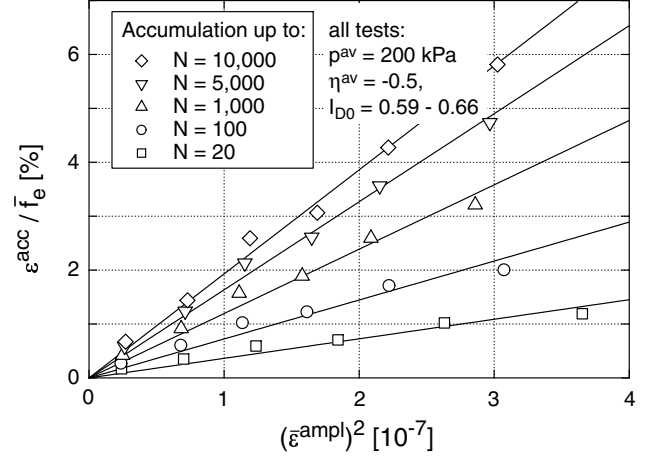
Fig. 5: Residual strain $\varepsilon^{\mathrm{acc}}$ normalized by f_e as a function of $(\varepsilon^{\mathrm{ampl}})^2$
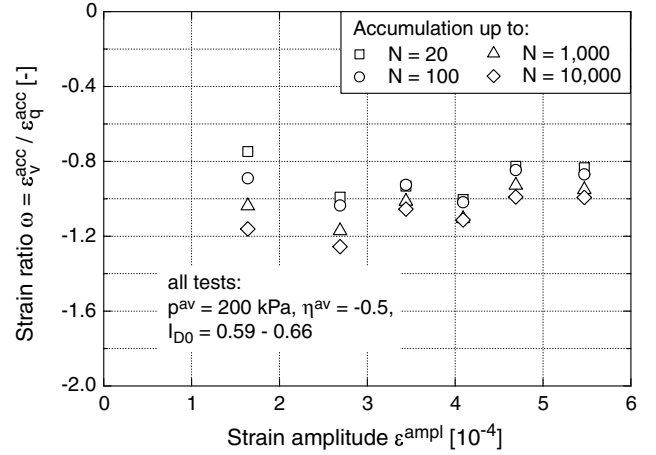
Fig. 6: Strain ratio ω as a function of the strain amplitude $\varepsilon^{\mathrm{ampl}}$ (mean value over 10^4 cycles)

2.3 Influence of the average mean pressure

Six tests with $\eta^{\mathrm{av}} = -0.5$, an amplitude ratio of $\zeta = q^{\mathrm{ampl}}/p^{\mathrm{av}} = 0.2$ and initial densities $0.62 \leq I_{D0} \leq 0.66$ were performed at different average mean pressures 50 kPa $\leq p^{\mathrm{av}} \leq 300$ kPa. The cyclic stress paths are shown in Fig. 7a and the strain amplitudes (mean values over 10^4 cycles) are presented in Fig. 8. The non-linear dependence of stiffness on pressure leads to an increase of the strain amplitudes with p^{av} for $\zeta = q^{\mathrm{ampl}}/p^{\mathrm{av}} = $ constant. From the shear strain amplitudes, Fig. 8, the stress-dependence of the hysteretic shear modulus was found to be $G_{\mathrm{hyst}} = \tau^{\mathrm{ampl}}/\gamma^{\mathrm{ampl}} \sim (p^{\mathrm{av}})^n$ with $n = 0.53$ (solid curve in Fig. 8).

Figure 9 presents the effect of p^{av} on the accumulated strain $\varepsilon^{\mathrm{acc}}$. The residual strains were normalized by f_{ampl} and f_e. Analogously to [2] the intensity of accumulation decreases with p^{av}. The exponential func-
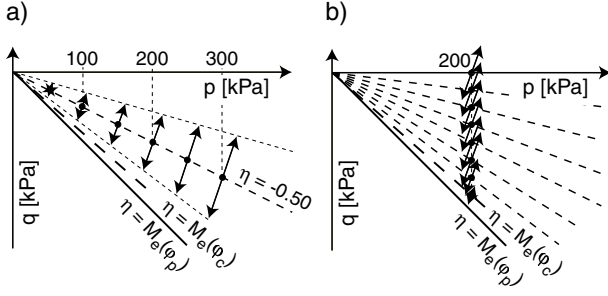
Fig. 7: Stress paths in the tests on the influence of the average stress: a) variation of p^{av}, b) variation of η^{av}

tion

$$f_p \;=\; \exp\left[-C_p\;(p^{\mathrm{av}}/p_{\mathrm{ref}}-1)\right] \tag{3}$$

with the reference pressure $p_{\mathrm{ref}} = p_{\mathrm{atm}} = 100$ kPa proposed in [2] remains valid for extension for 100 kPa $\leq p^{\mathrm{av}} \leq 300$ kPa, Fig. 9. The material constant $0.10 \leq C_p \leq 0.35$ was found to increase with N. In [2] it was demonstrated that this N-dependence can be neglected without noticeable aggravation of the accuracy of the acumulation model. For $\eta^{\mathrm{av}} = 0.75$ a value $C_p(N = 10^4) = 0.43$ was reported in [2], which is slightly higher than $C_p(N = 10^4) = 0.35$ for $\eta^{\mathrm{av}} = -0.5$. An application of Eq. (3) with $C_p = 0.43$ seems reasonable also for $q^{\mathrm{av}} < 0$. However, the accumulation rate at $p^{\mathrm{av}} = 50$ kPa was larger than it could be expected from the test results at higher pressures (Fig. 9, the test at $p^{\mathrm{av}} = 50$ kPa was repeated and similar rates were obtained). A more detailed study of the cumulative behaviour at small pressures $p^{\mathrm{av}} < 100$ kPa (for $\eta^{\mathrm{av}} < 0$ as well as for $\eta^{\mathrm{av}} \geq 0$) seems necessary. Similarly as for triaxial compression the direction of strain accumulation ω (cyclic flow rule) has been found to be independent of p^{av} (Fig. 10).
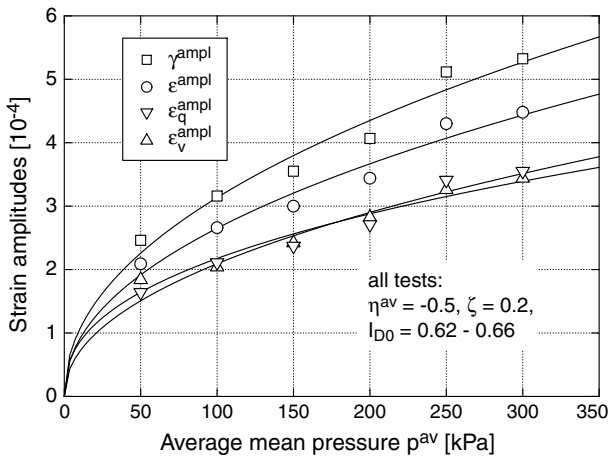
Fig. 8: Strain amplitudes (mean values over 10^4 cycles) in the tests with different average mean pressures p^{av}
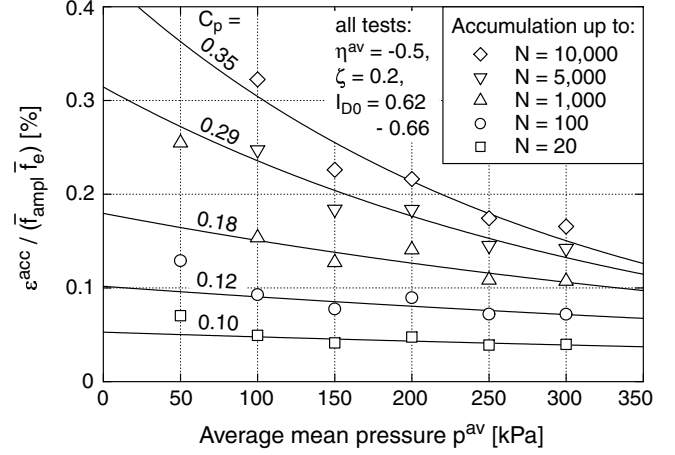
Fig. 9: Accumulated strain $\varepsilon^{\mathrm{acc}}$ normalized by f_{ampl} and f_e versus average mean pressure p^{av}
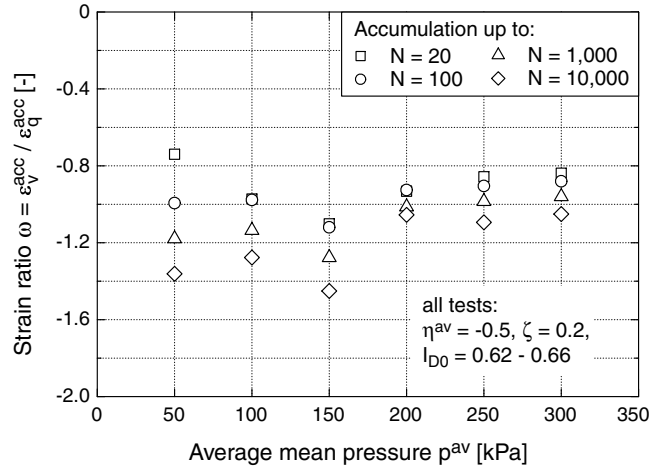
Fig. 10: Strain ratio ω as a function of the average mean pressure p^{av}

2.4 Influence of the average stress ratio

16 tests with $p^{\mathrm{av}} = 200$ kPa, initial densities $0.59 \leq I_{D0} \leq 0.65$ and different average stress ratios $-0.88 \leq \eta^{\mathrm{av}} \leq 1.0$ were performed. In most tests an amplitude ratio of $\zeta = q^{\mathrm{ampl}}/p^{\mathrm{av}} = 0.2$ was chosen. For $\eta^{\mathrm{av}} = -0.75$ and $\eta^{\mathrm{av}} = -0.88$ the amplitude ratio was reduced towards $\zeta = 0.1$ and $\zeta = 0.05$, respectively in order to keep the minimum deviatoric stress $q^{\mathrm{min}} = q^{\mathrm{av}} - q^{\mathrm{ampl}}$ above the failure line determined from monotonous tests. The stress paths of the tests with $\eta^{\mathrm{av}} \leq 0$ are shown in Fig. 7b.

In Fig. 11 the strain amplitudes in the tests with $\zeta = 0.2$ are plotted versus η^{av}. For triaxial compression the strain amplitudes decrease with $|\eta^{\mathrm{av}}|$ while for triaxial extension they increase with $|\eta^{\mathrm{av}}|$. While for $\eta^{\mathrm{av}} \geq 0$ the deviatoric strain amplitudes $\varepsilon_q^{\mathrm{ampl}}$ are significantly larger than the volumetric ones ($\varepsilon_v^{\mathrm{ampl}}$), this difference decreases with decreasing η^{av} and for $\eta^{\mathrm{av}} < -0.2$ both

amplitudes are almost identical. This reveals that for the amplitudes tested, the hysteretic stiffness significantly depends on the stress ratio η^{av}. This stress ratio dependence is usually less pronounced for smaller strain amplitudes (e.g. for $\gamma^{ampl} \leq 10^{-6}$ [4])
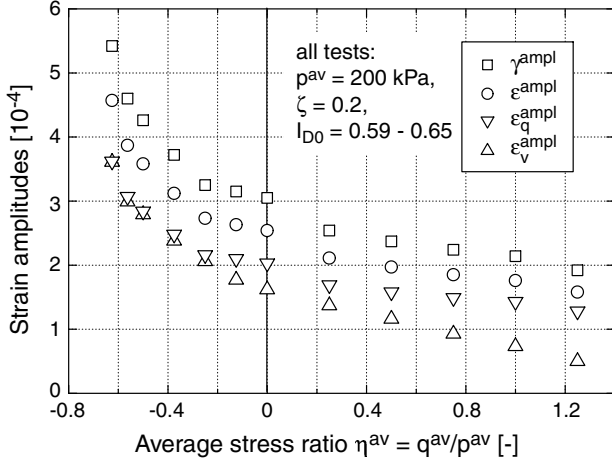
Fig. 11: Strain amplitudes as a function of the average stress ratio η^{av}

The dependence of the accumulated strain ε^{acc} on η^{av} is plotted in Fig. 12. The accumulation rate increases when the stress ratio $|\eta^{av}|$ increases, both for triaxial compression and extension. However, $\dot{\varepsilon}^{acc}(-\eta^{av}) \neq \dot{\varepsilon}^{acc}(\eta^{av})$, see Fig. 12.
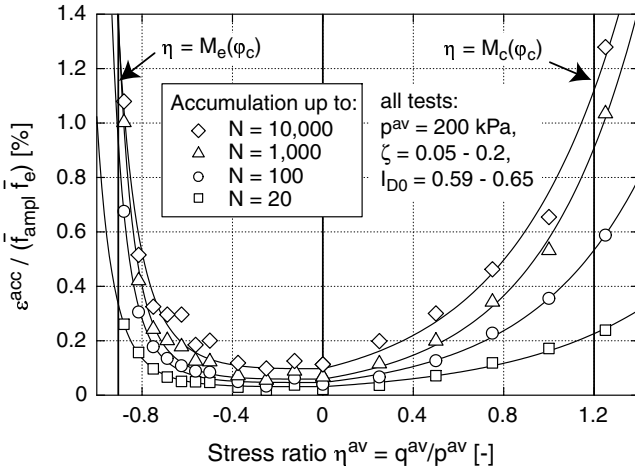
Fig. 12: Accumulated strain normalized by f_{ampl} and f_e versus average stress ratio η^{av}

In Fig. 13 $\varepsilon^{acc}/(f_{ampl}f_e)$ is plotted versus $\bar{Y}^{av}$, which is used as an alternative measure of the stress ratio [2]. At $\eta^{av} = 0$ the stress ratio is $\bar{Y}^{av} = 0$ and on the critical state line $\bar{Y}^{av} = 1$ holds. For the tests with $\eta^{av} \geq 0$ the function

$$f_Y \quad = \quad \exp\left(C_Y \, \bar{Y}^{av}\right) \tag{4}$$
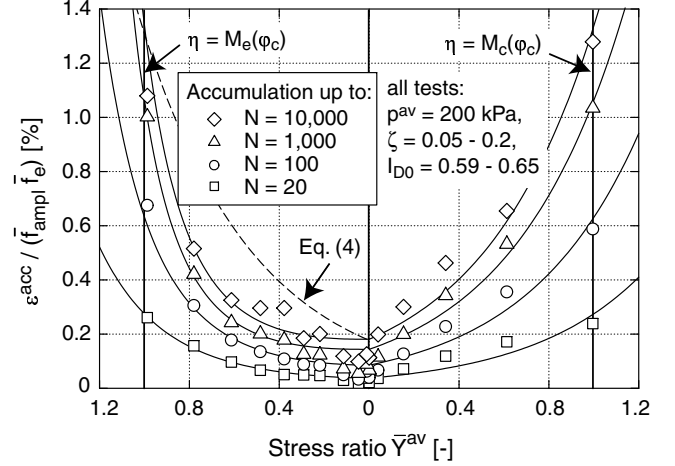
Fig. 13: Accumulated strain normalized by f_{ampl} and f_e versus average stress ratio $\bar{Y}^{av}$

could be fitted to the data resulting in $1.5 \leq C_Y \leq 2.0$ (solid lines in Fig. 13 at $\eta^{av} \geq 0$) which coincides well with $1.4 \leq C_Y \leq 2.1$ determined in [2]. However, the application of Eq. (4) with $C_Y = 2.0$ (proposed in [2]) to the tests with $\eta^{av} < 0$ overestimates the accumulation rates (in Fig. 13 this is shown for $N = 10^4$). In order to describe the tests with triaxial extension more precisely, a modification of Eq. (4) could be used:

$$f_Y \quad = \quad \exp\left[C_{Y1} \, (\bar{Y}^{av})^{C_{Y2}}\right] \tag{5}$$

A curve-fitting of Eq. (5) to the tests with $\eta^{av} \leq 0$ (solid lines in Fig. 13 at $\eta^{av} \leq 0$) resulted in $1.2 \leq C_{Y1} \leq 1.3$ and $2.3 \leq C_{Y2} \leq 2.7$. The material constants are therefore proposed as

$$C_{Y1} \quad = \quad \begin{cases} 2.0 & \text{for} \quad \eta^{av} \geq 0 \\ 1.25 & \text{for} \quad \eta^{av} < 0 \end{cases}$$

$$C_{Y2} \quad = \quad \begin{cases} 1.0 & \text{for} \quad \eta^{av} \geq 0 \\ 2.5 & \text{for} \quad \eta^{av} < 0 \end{cases}$$

However, Eq. (5) with the proposed constants still overestimates the accumulation rates in the tests with $-0.4 \leq \eta^{av} \leq 0$ (Fig. 13).

The following hypothesis could explain the difference between (4) and (5). It is based on the assumption that a static preloading (similarly as a cyclic preloading) of a sample reduces its rate of accumulation. Although, as yet, we have not collected sufficient experimental data for a quantitative description of this phenomenon, the qualitative observations seem plausible. The accumulation rate is slower for an isotropically preloaded sample (static preloading) compared to the accumulation rate of a freshly pluviated sample with the same stress and density (at the beginning of cyclic loading). It is not straightforward to determine the surface of static preloading for sands experimentally. Monitoring acoustic emissions (the intensity of grain cracking

or frictional contact changes) a surface similar to the one in Fig. 14 can be constructed [5]. For technical reasons the cyclic loading in the compression regime was preceded by the monotonic loading $0 \rightarrow 1 \rightarrow 2$ and in the extension regime by $0 \rightarrow 3 \rightarrow 4$. As we see, for small stress ratios in triaxial extension (dashed line) the cyclic loading is performed in a "overconsolidated state" and therefore the observed accumulation is slower than for an analogous stress ratio in compression. This could be responsible for the unsymmetry in the diagrams in Figs. 12 and 13. For larger stress ratios in extension, the average stress is "normally consolidated" and therefore the rates of accumulation are similar to the ones of triaxial compression.
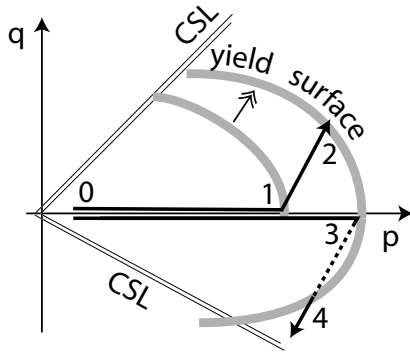
Fig. 14: Surface of static preloading and stress paths in the cyclic tests

The observed difference in the cumulative behaviour for triaxial compression and extension may be also attributed to an influence of the direction of deposition in respect to the directions of the major and the minor principal stresses. In the triaxial compression tests the major principal stress is parallel to the direction of deposition while it is perpendicular in the case of triaxial extension. The influence of the direction of deposition and the polarization of cyclic loading will be studied more detailed in future.

In Fig. 15a for the tests with $\eta^{av} \leq 0$ the strain ratio $\omega = \varepsilon_v^{acc}/\varepsilon_q^{acc}$ is plotted versus the average stress ratio η^{av}. For small values of $|\eta^{av}|$ the presentation of the reciprocal value $1/\omega = \varepsilon_q^{acc}/\varepsilon_v^{acc}$ in Fig. 15b is more convenient. As in the tests reported in [2] the direction of strain accumulation becomes more deviatoric (i.e. $|\omega|$ decreases) with an increasing obliquity of the average stress. While at an average stress lying on the p-axis ($\eta^{av} = 0$) the accumulation is pure volumetric ($\dot{\varepsilon}_q^{acc} = 0$, $\omega \rightarrow \infty$), a pure deviatoric accumulation ($\dot{\varepsilon}_v^{acc} = 0$, $\omega = 0$) is obtained on the critical state line ($\eta^{av} = M_e(\varphi_c) = -0.88$). For $\eta^{av} > M_e(\varphi_c)$ cyclic loading leads to a densification of the material, at an average stress beyond the CSL ($\eta^{av} < M_e(\varphi_c)$) a dila-

tive material behaviour is expected. As for $\eta^{av} \geq 0$ [2] the direction of strain accumulation can be well approximated by the flow rules of constitutive models for monotonous loading (modified Cam clay model, hypoplastic model, Fig. 15).
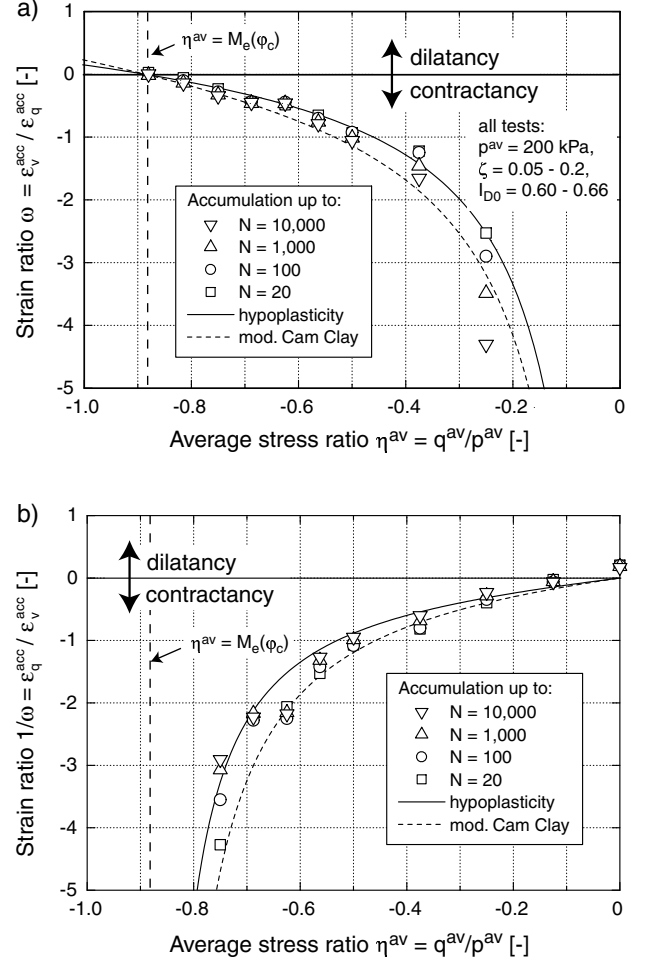
Fig. 15: a) Strain ratio $\omega = \varepsilon_v^{acc}/\varepsilon_q^{acc}$ and b) reciprocal value $1/\omega = \varepsilon_q^{acc}/\varepsilon_v^{acc}$ as a function of the average stress ratio η^{av}, comparison with the flow rules of the modified Cam clay model and the hypoplastic model

Fig. 20 in [2] has been extended by now covering the tests with $\eta^{av} \leq 0$, Fig. 16. The direction of strain accumulation is shown as a unit vector in the p-q-plane starting at (p^{av}/q^{av}) with the inclination $1/\omega$ towards the horizontal. From Fig. 16 the strong dependence of the cyclic flow rule on the average stress ratio (and also the slight N-dependence) is obvious.

2.5   Influence of the number of cycles

Figure 17 contains the accumulation curves $\varepsilon^{acc}(N)$ measured in the tests on the influence of ε^{ampl}, p^{av} and η^{av} normalized with f_{ampl}, f_e, f_p and f_Y (Eq. (5)). The tests with $-0.4 \leq \eta^{av} \leq 0$ were excluded from Fig. 17
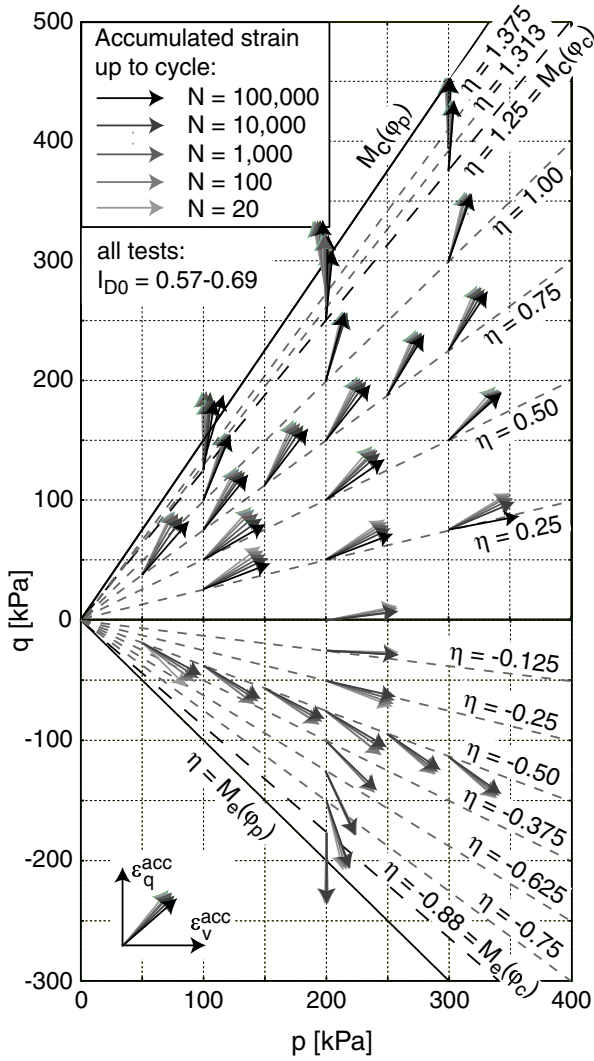
Fig. 16: Direction of accumulation in the p-q-plane: tests with different average stresses $\boldsymbol{\sigma}^{\mathrm{av}}$

Fig. 17: Accumulation curves $\varepsilon^{\mathrm{acc}}(N)$ normalized with f_{ampl}, f_p, f_Y and f_e

- The direction of accumulation does not depend on the strain amplitude $\varepsilon^{\mathrm{ampl}}$ and on the average mean pressure p^{av}. The cyclic flow rule is a simple function of the average stress ratio $\eta^{\mathrm{av}} = q^{\mathrm{av}}/p^{\mathrm{av}}$ only and can be well approximated by the flow rules of constitutive models for monotonous loading [2].

- The intensity of accumulation $\dot{\varepsilon}^{\mathrm{acc}} = \partial \varepsilon^{\mathrm{acc}}/\partial N$ increases proportionally to the square of the strain amplitude $\varepsilon^{\mathrm{ampl}}$ and decreases exponentially with p^{av}. The validity of the functions f_{ampl}, f_p and f_N found in the tests with triaxial compression [2] and implemented into the accumulation model [1] could be extended to $q^{\mathrm{av}} < 0$.

- The accumulation rate $\dot{\varepsilon}^{\mathrm{acc}}$ increases if the average stress ratio $|\eta^{\mathrm{av}}|$ increases, but $\dot{\varepsilon}^{\mathrm{acc}}(-\eta^{\mathrm{av}}) \neq \dot{\varepsilon}^{\mathrm{acc}}(\eta^{\mathrm{av}})$. A modification of the function f_Y for $\eta^{\mathrm{av}} < 0$ was proposed in this paper, but two alternative explanations of this effect are still to be examined.

Acknowledgements

References

[1] Niemunis A, Wichtmann T, Triantafyllidis T. A high-cycle accumulation model for sand. Computers and Geotechnics, 2005;32(4):245-263.

(see the remarks in Sec. 2.4) and a test with $N = 50,000$ cycles at $p^{\mathrm{av}} = 200$ kPa, $\eta^{\mathrm{av}} = -0.5$ and $I_{D0} = 0.63$ was added. Mostly all normalized accumulation curves fall into the bandwidth of the tests presented in Fig. 28 of [2]. Therefore, the approximation

$$f_N \;\; = \;\; C_{N1}\left[\ln(1 + C_{N2}N) + C_{N3}N\right] \qquad (6)$$

with the material constants $C_{N1} = 3.4 \cdot 10^{-4}$, $C_{N2} = 0.55$ and $C_{N3} = 6.0 \cdot 10^{-5}$ (solid curve in Fig. 17 and in Fig. 28 of [2]) is justified also for triaxial extension.

3   Summary and conclusions

Numerous drained cyclic tests with triaxial extension ($q^{\mathrm{av}} < 0$) have been performed and compared to cyclic tests at $q^{\mathrm{av}} \geq 0$ published in [2]. The main findings are:

[2] Wichtmann T, Niemunis A, Triantafyllidis T. Strain accumulation in sand due to cyclic loading: drained triaxial tests. Soil Dynamics and Earthquake Engineering (in print).

[3] Wichtmann T, Niemunis A, Triantafyllidis T. The effect of volumetric and out-of-phase cyclic loading on strain accumulation. Cyclic Behaviour of Soils and Liquefaction Phenomena, Proc. of CBS04, Bochum, March/April 2004, Balkema, 2004:247-56.

[4] Wichtmann T, Triantafyllidis T. Influence of a cyclic and dynamic loading history on dynamic properties of dry sand, part II: cyclic axial preloading. Soil Dynamics and Earthquake Engineering, 2004;24(11):789-803.

[5] Tanaka Y. New findings in recent experimental studies, In: Oda M, Iwashita K. Mechanics of Granular Materials, Balkema, Rotterdam, 1999;270:276.